Surface states, surface potentials, and segregation at surfaces of tin-doped In_2O_3

Y. Gassenbauer, R. Schafranek, and A. Klein*
Darmstadt University of Technology, Institute of Materials Science, Petersenstrasse 23, D-64287 Darmstadt, Germany

S. Zafeiratos, M. Hävecker, A. Knop-Gericke, and R. Schlögl
Fritz-Haber Institut, Department of Inorganic Chemistry, Faradayweg 4-6, 14195 Berlin, Germany
(Received 7 February 2006; revised manuscript received 19 April 2006; published 9 June 2006)

Surfaces of In_2O_3 and tin-doped In_2O_3 (ITO) were investigated using photoelectron spectroscopy. Parts of the measurements were carried out directly after thin film preparation by magnetron sputtering without breaking vacuum. In addition samples were measured during exposure to oxidizing and reducing gases at pressures of up to 100 Pa using synchrotron radiation from the BESSY II storage ring. Reproducible changes of binding energies with temperature and atmosphere are observed, which are attributed to changes of the surface Fermi level position. We present evidence that the Fermi edge emission observed at ITO surfaces is due to metallic surface states rather than to filled conduction band states. The observed variation of the Fermi level position at the ITO surface with experimental conditions is accompanied by a large apparent variation of the core level to valence band maximum binding energy difference as a result of core-hole screening by the free carriers in the surface states. In addition segregation of Sn to the surface is driven by the surface potential gradient. At elevated temperatures the surface Sn concentration reproducibly changes with exposure to different environments and shows a correlation with the Fermi level position.

DOI: 10.1103/PhysRevB.73.245312 PACS number(s): 73.20.At, 68.35.Dv, 79.60.Bm, 68.47.Gh

I. INTRODUCTION

Tin-doped indium oxide (In_2O_3:Sn or ITO) is a degenerately doped semiconductor with a high transparency in the visible optical regime.[1,2] Its high electron concentration of up to $\sim 10^{21}$ cm^{-3} is obtained by substitutional doping with Sn. However, it is mentioned that most of the Sn atoms form neutral defect complexes with interstitial oxygen atoms forming reducible and nonreducible defect complexes.[3–6] ITO is largely used as a transparent electrode in optoelectronic thin film devices as e.g. flat-panel displays, organic light emitting diodes (OLEDs),[7] and organic photovoltaic cells (OPVs),[8,9] but also as sensor material.[10] For these applications the electric surface potentials (Fermi level and vacuum level) are important.[11,12]

The work function ϕ of a material can change, in principle, due to variation of the surface dipole and, for semiconducting materials, when the Fermi level E_F at the surface varies by bending of the bands (see, e.g., Ref. 13). The different contributions to changes of the work function are illustrated in Fig. 1. Work function and surface Fermi level position can both be directly determined using x-ray and ultraviolet photoelectron spectroscopy (XPS and UPS) if a sufficient electrical contact between the sample surface and the spectrometer system is maintained.[13] Then the Fermi energy is determined directly from the Fermi edge emission of any metallic sample and the work function is derived from the electrons with zero kinetic energy at the secondary electron cutoff. A shift of the valence and conduction band edges (E_{VB} and E_{CB}) with respect to the Fermi level due to band bending is indicated by a rigid shift of the complete spectra including all core levels, valence bands, and also the secondary electron cutoff. A change of the surface dipole without altering the surface Fermi level position only shifts the secondary electron cutoff.

The surface potentials of ITO have been investigated by many researchers mainly with a focus on the determination and modification of its work function (see Refs. 14–23 and references therein). Interest in the ITO surface potentials was induced by the observation that an increase of the ITO work function leads to a desired lower injection barrier for holes at the interface with organic conductors. This increase in work function is typically achieved by oxidative treatments such as oxygen plasma, UV ozone, or chemical treatments.

The use of ITO in OLEDs combines two apparently excluding properties: The bulk of ITO needs to be as conducting as possible requiring a Fermi level as high as possible with respect to the band edges or the vacuum level. In contrast, a low injection barrier is reached by a Fermi level at the interface to the organic conductor as low as possible. Obviously both features can be combined using ITO, while other

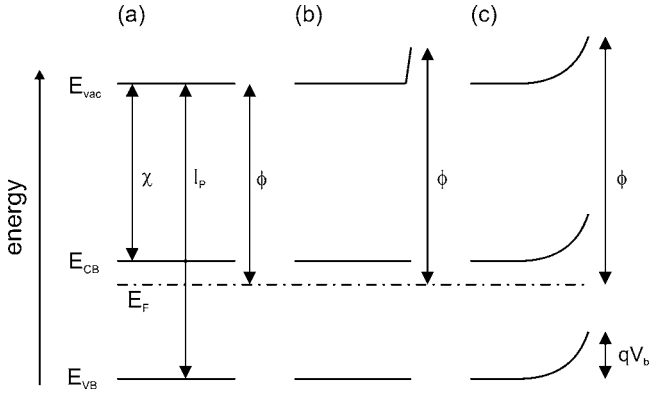

FIG. 1. Surface potentials of an *n* type semiconductor in flat band condition (a). The work function ϕ can change either by modification of the surface dipole preserving flat bands but modifying the electron affinity χ and ionization potential $I_P=\chi+E_g$ (b). The work function might also change by bending of the bands at the surface qV_b (c). Surface dipole and band bending could also change simultaneously.

highly conducting transparent oxides (TCOs) as doped SnO_2, ZnO, and CdO are typically not used in OLEDs, which might be due to the fact that these do not simultaneously fulfill these criteria.

Most of the work performed on work function of ITO does not distinguish between changes in Fermi level and surface dipole as origin of the work function changes. To our knowledge only Christou *et al.*[22] and Lee *et al.*[23] point out that the ~0.4 eV changes in work function of their differently treated samples are in parallel to the shift of the valence band maximum and core levels, thus leaving the electron affinity χ, defined as the energy difference between vacuum level and conduction band minimum (see Fig. 1), unchanged. As in earlier work,[24] the shift of the binding energies were interpreted by Christou *et al.* in terms of a flat band model similar to the one shown in Fig. 1(a), but with the Fermi level inside the conduction band.[22] The lowering of the Fermi level after oxidative treatment was attributed to a reduction of the doping level near the surface by incorporation of oxygen in the lattice. In contrast, Lee *et al.* attribute the work function and Fermi level changes to a change of surface band bending.[23] However, no explanation for the origin of the band bending and its modification are given.

ITO thin films deposited *in situ* by radio frequency magnetron sputtering exhibit changes of up to ~1 eV in XPS binding energies depending on deposition conditions.[25–27] The Fermi level in these measurements is found as low as ~2.2 eV above the valence band maximum for the most strongly oxidized samples (see also results presented below). These large shifts are interpreted in terms of a surface depletion layer as sketched in Fig. 1(c). A similar explanation has been given for surface properties of reactively evaporated In_2O_3 films.[28,29]

The different interpretation of surface potential data (see Refs. 22–29) is directly related to the nature and magnitude of the band gap of ITO and therefore to the energy of the conduction band minimum. Conduction band states of semiconductors are usually not occupied with electrons and cannot be directly measured using photoemission. However, UP spectra of ITO surfaces frequently show an emission at the Fermi energy.[16,22,24,26,27] This has been attributed to emission from filled conduction band states, which seems to be straightforward for a degenerately doped semiconductor with a partially filled conduction band.[16,22,24] In XPS and UPS the valence band maximum energy of highly doped ITO is typically found at values $E_F - E_{VB} \approx 3$ eV.[22,24,25,27] If the observed electronic states at the Fermi energy are due to conduction band states this would indicate a band gap smaller than ~3 eV. An indirect band gap of $E_{g,i}=2.6$ eV has been reported for single crystal In_2O_3,[30] which would agree with this assignment. Recent scanning tunneling spectroscopy and optical measurements also indicate an indirect band gap of 2.4 eV.[31]

Such a small fundamental band gap is unlikely, since highly doped ITO samples show a considerable blueshift of the absorption edge due to the occupation of conduction band states.[1] The effect is known as Burstein-Moss shift[32,33] and has also been observed for ITO films prepared under the same conditions as the ones used for this study.[25] Absorption edges above 4 eV mean that the Fermi level is $\gtrsim$4 eV above the valence band maximum. This contrasts XPS/UPS observations, which reproducibly find the valence band maximum $\lesssim$3.5 eV below the Fermi level (see Refs. 22–27 and data given below). If the fundamental gap of ITO is 2.6 eV, then the Fermi level would be $E_F - E_{CB} \gtrsim 1.4$ eV above the conduction minimum for the highest doped films, no matter if the band gap is direct or indirect. Assuming a constant effective mass in the conduction band, the electron concentration can be calculated according to

$$n = \frac{1}{3\pi^2}\left(\frac{2m^*(E_F - E_{CB})}{\hbar^2}\right)^{3/2}. \quad (1)$$

Using $m^*=0.35m_e$ for the effective mass in the conduction band of ITO[1] and a Fermi level position $E_F - E_{CB}=1.4$ eV results in an electron concentration of 1.6×10^{21} cm^{-3}. This value is larger than those observed experimentally for ITO.[1,2] Even larger values would result if the largest absorption edges of ~4.3 eV and band gap renormalization[22,34] would have been considered. It seems therefore more reasonable to identify the fundamental gap of In_2O_3 with the direct band gap of $E_{g,d}=3.75$ eV.[1] Theoretical *ab initio* band structure calculations also gave no hint for the existence of an indirect gap in In_2O_3.[35] Although the situation for ITO is more complex, mostly because of the filling of the conduction bands with electrons, the valence band maximum varies by less than 0.25 eV throughout the whole Brillouin zone in these calculations.[35] Any indirect band gap could therefore be not more than 0.25 eV smaller than the smallest direct one.

In this contribution we present a detailed study of the surface properties of In_2O_3 and ITO thin films using photoelectron spectroscopy. The results will also provide an explanation for the different band gaps observed. In a first part we show results from ITO thin films measured directly after deposition without breaking vacuum, thereby avoiding surface contaminations and the need for post-deposition surface treatments. The second part describes results obtained from measurements performed *in situ* during exposure of ITO films to high pressures (up to several 100 Pa) of oxidizing and reducing species. The measurements provide evidence for the presence of surface states as origin of the emission at the Fermi edge and the existence of a surface carrier depletion layer. Significant evidence will be derived from the observation of Sn segregation. In particular, the reproducible changes in surface Sn concentration with Fermi level position induced by changing the environment highlight the new value added by the possibility to perform XPS studies at higher pressures. Such measurements are particularly important since ITO can also be used as gas sensing material.[10] The gas sensing effect is generally expected to be caused by changing the position of the Fermi level at the surface due to adsorption and desorption of oxidizing or reducing species.[12] Hence, ITO should not only show a surface depletion layer, but the surface Fermi level position should also vary with gas environment. The detection of surface potential changes in gas environment is not straightforward, since the photoemission technique usually requires a vacuum environment with pressures below 10^{-5} Pa, which is much lower than the pressures exposed to sensors.

II. EXPERIMENTAL

Experiments in Darmstadt were carried out in the Darmstadt Integrated System for Materials Research (DAISYMAT), which combines several thin film deposition chambers with a multitechnique surface analysis system.[26,36] Thin films of In_2O_3 and ITO were deposited by radio frequency magnetron sputtering from ceramic targets. X-ray diffraction of films deposited onto glass substrates exhibit only the In_2O_3 bixbyite phase[37] as generally observed for sputter deposited In_2O_3 and ITO films.[2] Glass substrates coated with conducting fluorine-doped SnO_2 were used for XPS measurements to avoid binding energy shifts due to charging effects. The ITO target is composed of 90 wt % In_2O_3 and 10 wt % SnO_2, which corresponds to 17 mol % SnO_2, or to a 9.2% contribution of Sn to the total cation content ([Sn]/([Sn]+[In])). A total gas pressure of 0.5 Pa at variable argon to oxygen ratios was used. Electrical and optical properties of the ITO films are described elsewhere.[25,27] ITO films deposited at 400 °C substrate temperature in pure argon show resistivities of $\sim 2\times 10^{-4}$ Ω cm and high optical transparency.

X-ray and UV photoelectron spectroscopy measurements performed after thin film deposition were carried out using a Physical Electronics PHI 5700 spectrometer system. Monochromatic Al Kα radiation ($h\nu$=1486.6 eV) has been used as excitation for XPS. At 5.85 eV pass energy the PHI system provides an overall experimental resolution better than 400 meV for XPS measurements as determined by the Gaussian broadening of the Fermi edge of a clean Ag sample. The spectrometer is calibrated at regular intervals by determining the core-level binding energies of copper [BE(Cu2$p_{3/2}$)=932.7 eV], silver [BE(Ag3$d_{5/2}$)=368.3 eV], and gold [BE(Au4$f_{7/2}$)=84.0 eV] with respect to the Fermi energy.

Photoemission experiments at higher pressures were performed at the U49/2-PGM 2 undulator beamline of the BESSY II storage ring, which supplies photons in the energy range $h\nu$=90–1500 eV.[38] The photoelectron spectrometer system uses a differentially pumped lens system.[39,40] ITO films prepared at 400 °C substrate temperature with pure Ar as sputter gas have been used for the experiments. Samples were heated using light from a laser diode array fed into the vacuum system with a glass fiber and placed ~2 mm before the entrance slit of the electron lens system. All spectra were recorded in normal emission. Hydrogen and oxygen gas was dosed via leak valves. For measurements at pressures above 0.1 Pa, the pumping speed was reduced by closing the valve between the measurement chamber and the turbomolecular pump. Residual pumping was thereby maintained through the small entrance slit of the lens system. Pressures were measured using a Pfeiffer PKR full range gauge at lower pressures and a Baratron at higher pressures.

Most of the spectra were recorded using a photon energy of $h\nu$=600 eV, which has been selected as a compromise between accessibility of all core lines, surface sensitivity, and reasonable photoionization cross sections. It was tried to avoid changing of the excitation energy because of the importance of energy calibration, which might differ slightly after moving the monochromator. The overall spectral resolution at 600 eV is better than 200 meV. Binding energies are calibrated using the Fermi edge emission, which is occasionally observed on ITO surfaces.[16,22,26,27] The position of the Fermi edge has been found to be reproducible within ±0.05 eV, which is important for a reliable binding energy calibration. Intensities of the spectra are normalized with respect to the current in the electron storage ring.

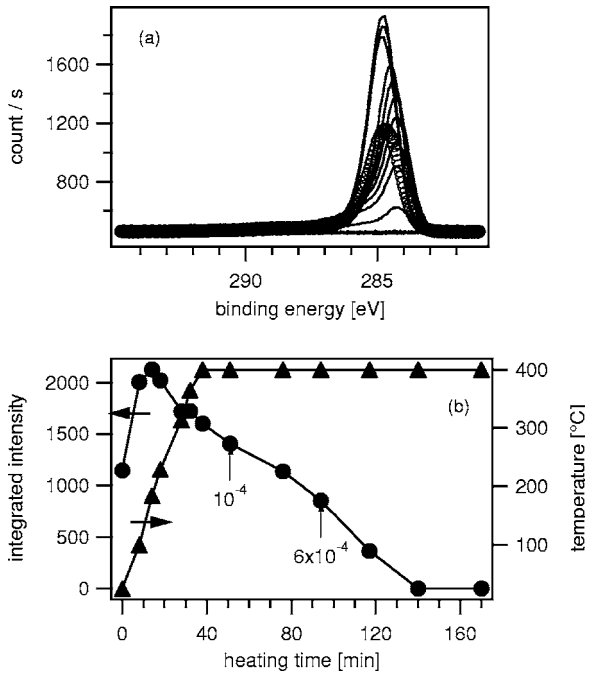

FIG. 2. Carbon 1s core level spectra taken during heating of an ITO thin film sample stored in air (a). The first spectrum recorded at room temperature is shown by circles. Small arrows indicate the time where oxygen has been introduced into the chamber. The corresponding pressures are given in mbar. The intensity of the C 1s line in dependence on time is shown in (b) together with the temperature of the substrate.

In total we have investigated three ITO samples at higher pressures, which were all deposited ~2 weeks before the measurements onto oxidized Si wafers at 400 °C substrate temperature in pure Ar. The samples were mounted on a sample holder and a thermocouple was attached to it. All observed changes in binding energy and peak shape were highly reproducible. Since the samples for high pressure measurements were prepared in a separate deposition chamber which was not connected to the analysis system, the sample surfaces are contaminated and therefore show a noticeable C 1s emission line. The C 1s emission monitored during heating of a sample in 6×10^{-2} Pa oxygen is shown in Fig. 2(a). Its intensity as a function of heating time is shown in Fig. 2(b). The approximate doubling of the C 1s intensity after initial heating to ~200 °C has been reproducibly observed on different samples. A possible explanation for the striking increase in C 1s intensity could be that the (hydrocarbon) contaminations are originally adsorbed as three-dimensional aggregates, which spread over the surface during heating.

Further heating of the sample leads to a reduction of the C 1s intensity. After ~2 h at a temperature of 400 °C, no more

carbon was detected on the surface. The surface remained free of carbon during the complete subsequent experiment, which has frequently been checked by recording the C 1*s* signal. Cleaning of other substrates could take less time or eventually also higher temperatures of up to 500 °C for SnO_2 samples. In principle, the details of the surface cleaning warrant a more detailed description because of their importance for gas sensing effects and the produced surface condition. However, this is not within the scope of the present publication. Although surface contaminations with hydrocarbons can be excluded, the data presented in this contribution also indicate that there are differences between the freshly deposited samples and those which were heat cleaned.

III. RESULTS

A. Thin film deposition

Core-level and valence band spectra of sputter deposited ITO and In_2O_3 thin films are shown in Fig. 3. The displayed spectra were selected since these show the largest differences in binding energy. Substrate temperatures during deposition were 400 °C for ITO and 200 °C as well as 400 °C for In_2O_3, respectively. The intensity ratio between indium and oxygen does not vary significantly with substrate temperature and oxygen pressure during deposition. In addition no metallic In or Sn components are observed in any of the spectra.

The O 1*s* level of the In_2O_3 films exhibits an additional structure at higher binding energy. The origin of it is not fully clear yet. According to the binding energy of ~532 eV it could be attributed either to hydroxide[21] but also to a peroxolike surface species.[41,42] Since the high binding energy component is absent for the ITO samples, the latter explanation seems to be more probable. It further agrees with a recent calculation of In_2O_3 surface properties.[42]

Apart from binding energy shifts, which will be discussed below, the valence band spectra in Fig. 3 show three noticeable differences: (i) the sample showing the largest binding energies (a) shows emission on the low binding energy side of the valence band maximum at binding energies 2–3 eV. Such emissions have also been observed at reduced In_2O_3 and SnO_2 surfaces and can be attributed to the presence of partially unsaturated cations;[28,43–47] (ii) The same sample (a) shows a emission at the Fermi energy, which is more clearly seen in UP spectra. With increasing oxygen content in the sputter gas the valence band emissions shift to lower binding energies. Simultaneously the Fermi edge emission disappears (see also Refs. 26 and 27). No Fermi edge emission is observed for any of the In_2O_3 samples, neither in XPS nor in UPS.

The binding energy of the valence band maximum with respect to the Fermi energy BE(VB), which corresponds to the distance between the Fermi energy E_F and the valence band maximum energy E_{VB} in Fig. 1, are determined from the linear extrapolation of the leading valence band emission to the background given by the defect states in the band gap as indicated on the spectra in Fig. 3. Binding energies of the In 3*d* [BE(In 3*d*)] and O 1*s* [BE(O 1*s*)] core levels are determined from the maxima of the emissions with respect to the Fermi energy. The spectra exhibit significantly different binding energies. Although the shifts of the In 3*d*, O 1*s*, and valence band onset between the differently prepared samples are in the same direction, they are not of the same magnitude (see Table I). The different magnitude of the shifts corresponds to a variation of the core level (CL) to valence band maximum binding energy difference $BE_{VB}(CL)$, given by $BE_{VB}(CL)=BE(CL)-BE(VB)$, where CL=In $3d_{5/2}$ or O 1*s*, respectively. The corresponding values for BE_{VB}(In 3*d*) and BE_{VB}(O 1*s*) are included in Table I.

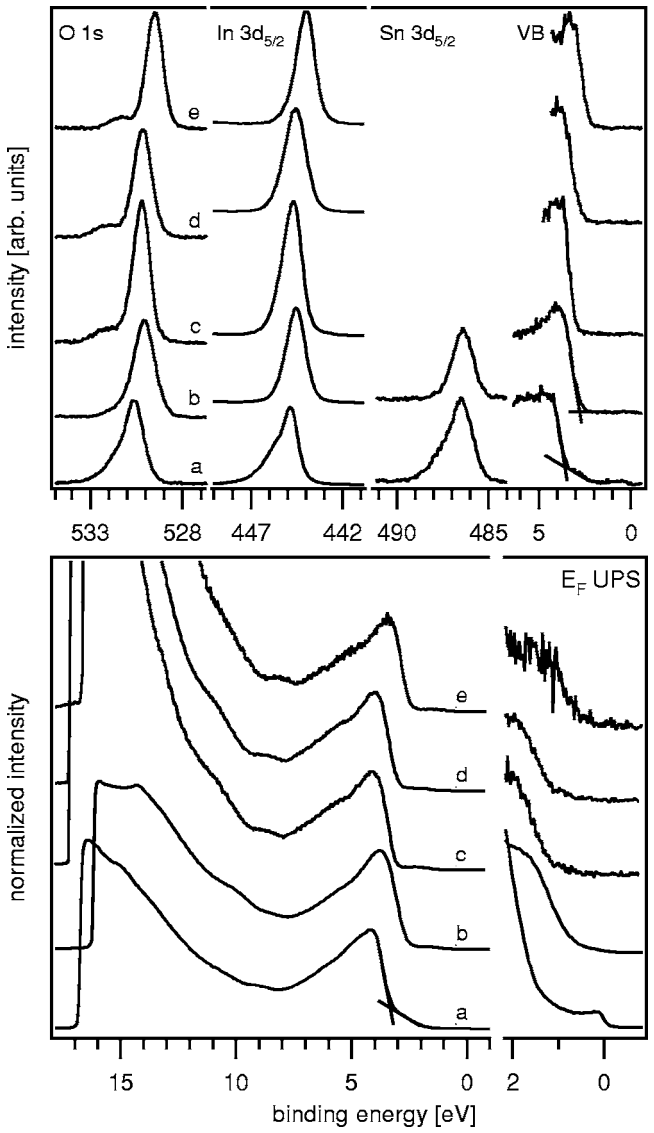

FIG. 3. X-ray photoelectron core level and valence band spectra (top) and UPS spectra (bottom) of ITO (a,b) and In_2O_3 (c–e) thin films prepared by radio frequency magnetron. Substrate temperatures were 400 °C for samples (a–c) and 200 °C for samples (d) and (e), respectively. The films were deposited with pure Ar (a,c,d) and with a 90/10 Ar/O_2 gas mixture (b,e). A magnified view of the UPS spectra close to the Fermi energy (zero binding energy) is also shown (E_F UPS). In this part of the figure the intensity at binding energies $\gtrsim$1 eV are mostly due to excitation of valence band states by a satellite of the He discharge lamp.

TABLE I. Substrate temperature (T_{sub}), oxygen fraction in sputter gas (O_2), binding energies of core levels BE(In $3d_{5/2}$), BE(O 1s), and valence band maximum BE(VB) as well as work function ϕ for differently prepared In_2O_3 and ITO thin films. Binding energies of core levels are determined from the maximum of the peaks with uncertainties ±0.05 eV. The valence band edge is derived from the intersection of the linear extrapolation of the leading edge of the valence bands with similar uncertainties. The core-level to valence band maximum binding energy differences $BE_{VB}(In\ 3d) = BE(In\ 3d_{5/2}) - BE(VB)$ and $BE_{VB}(O\ 1s) = BE(O\ 1s) - BE(VB)$ and the electrical conductivity σ are also given. Unless units are given, all values are in electron Volts.

Film	T_{sub} [°C]	O_2 [%]	BE(In $3d_{5/2}$)	BE(O 1s)	BE(VB)	ϕ	BE_{VB}(In $3d$)	BE_{VB}(O 1s)	σ [S/cm]
ITO	400	0	444.87	530.54	3.54	4.47	441.33	527.00	4550
ITO	400	1	444.63	530.23	2.94	4.83	441.69	527.29	1620
ITO	400	2	444.49	530.08	2.73	5.04	441.76	527.35	395
ITO	400	3	444.48	530.06	2.69	5.16	441.79	527.37	150
ITO	400	4	444.51	530.09	2.76	5.11	441.75	527.33	47
ITO	400	5	444.39	529.96	2.67		441.72	527.29	56
ITO	400	6.5	444.37	529.94	2.60	5.2	441.77	527.34	20
ITO	400	10	444.49	530.06	2.64	5.05	441.85	527.42	18
In_2O_3	400	0	444.71	530.26	2.98	3.98	441.73	527.28	40
In_2O_3	200	0	444.58	530.10	2.69	3.97	441.89	527.41	11
In_2O_3	200	10	443.97	529.49	2.26	4.58	441.71	527.23	2

Because of the different magnitude of the binding energy shifts for different emissions it is not straightforward to attribute them to a shift of the Fermi level. Nevertheless, this seems to be reasonable, since the Sn-doped samples show larger binding energies (higher Fermi level position) than the undoped ones and films deposited in pure argon have larger binding energies than films deposited with additional oxygen. Furthermore, there is a direct correlation of binding energies (Fermi level positions) with electrical conductivities, which are also included in Table I. However, it remains to be identified which of the levels is to be used to quantify the Fermi level shift and therefore the origin of the variation in BE_{VB}(CL) needs to be understood.

The O 1s, In 3d, and Sn 3d core levels of the ITO film deposited with pure argon show a strong asymmetric shape. All other core levels are almost symmetric. We observe comparable asymmetries for highly degenerate Al-doped ZnO as well as for Sb- and F-doped SnO_2. Because of our *in situ* preparation, we do not consider adsorbates, which can also lead to considerable modifications of the peak shape,[21] as origin of the asymmetry. This is also supported by the complete absence of carbon emissions. To model the line shapes we have therefore used an approach which is based on interactions of the photoelectron and the core hole with conduction electrons,[48] which has already been applied in the literature to model the line shape of core levels of highly doped oxides, in particular also for ITO.[22,45] The idea is that the conduction electrons screen the core hole in the photoemission process giving rise to a "screened" component at lower binding energy. This main line is accompanied by satellites at higher binding energies due to inelastic losses by excitation of one or more plasmons in the degenerate electron gas. Since the electron density in the electron gas is significantly lower than in bulk metals, the plasmon frequency is also considerably smaller and amounts only to $\lesssim 1$ eV.[1]

Least-squares fits of the In $3d_{5/2}$ and O 1s lines of the spectra (a) in Fig. 3 are presented in Fig. 4. In contrast to the model used by Christou *et al.*,[22] we have used three Voigt components with energy spacings ΔE and $2 \times \Delta E$, which better describe the experimental curves. To reduce fitting pa-

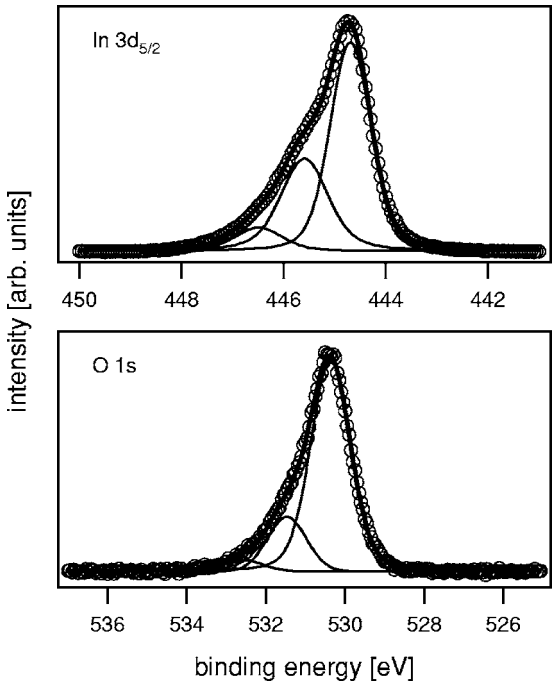

FIG. 4. Line fits of the In $3d_{5/2}$ and O 1s lines recorded with monochromatic Al Kα radiation from an ITO thin film deposited at 400 °C substrate temperature in pure argon [spectra (a) in Fig. 3]. The energy difference between the three components is identical. Intensity ratios are 1 : 0.55 : 0.14 for In 3d and 1 : 0.23 : 0.05 for O 1s, respectively.

rameters the satellite lines are assumed to have the same width and Gauss-Lorentz ratio as the main line. A good agreement with experimental data is obtained for both levels. The energy spacings of the main lines and the satellite lines are determined as $\Delta E = 0.89 \pm 0.05$ and $\Delta E = 1.10 \pm 0.05$ eV for In 3*d* and O 1*s*, respectively. Intensity ratios ΔI of the main peak to the two satellite lines are 1 : 0.55 : 0.14 for In 3*d* and 1 : 0.23 : 0.05 for O 1*s*.

Using the values for the energy splitting ΔE and intensity ratios ΔI a weighted average (baricenter) of the binding energy of the peak can be calculated.[22,45] This corresponds to the unrelaxed "Koopmanns" photoemission final state, which is projected onto the screened and unscreened final state. The baricenter is shifted with respect to the screened component by

$$\Delta \mathrm{BE} = (\Delta E \Delta I_1 + 2 \times \Delta E \Delta I_2)/(1 + \Delta I_1 + \Delta I_2), \qquad (2)$$

where the subscripts 1 and 2 refer to the two satellite components. The analysis results in $\Delta \mathrm{BE} = 0.48$ and 0.28 eV for the In 3*d* and the O 1*s* levels. The difference between the binding energy of the screened component and the maxima of the In 3*d* and O 1*s* emission are −0.05 and −0.03 eV, respectively. The peak maxima have been determined by fitting a Gaussian profile to the data points around the maximum and correspond to the binding energies in Fig. 5 and Table I. With these difference the baricenters of the peaks are shifted with respect to the peak maxima by 0.43 and 0.25 eV for In 3*d* and O 1*s*, respectively. This difference almost equals the observed variation of the core level to valence band maximum binding energy differences for the different samples (doping levels), as also described in the literature.[45]

Figure 5 shows the dependence of the In $3d_{5/2}$ core level to valence band maximum binding energy difference $\mathrm{BE_{VB}}$(In 3*d*) on the binding energy of the valence band maximum BE(VB). Within the experimental uncertainty the values for In_2O_3 are constant with $\mathrm{BE_{VB}}(\mathrm{In}\ 3d) = 441.8 \pm 0.1$ eV. For ITO films the same value is observed for lower doped films with $\mathrm{BE(VB)} \lesssim 3$ eV. For larger values of BE(VB) a significant decrease of $\mathrm{BE_{VB}}$(In 3*d*) by up to 500 meV is observed.

The different behavior of $\mathrm{BE_{VB}}$(In 3*d*) for undoped and Sn doped In_2O_3 suggests that the Sn content affects the surface properties. Differences between ITO and In_2O_3 are also obvious from UP spectra as the latter do not show a clear Fermi edge emission. Furthermore, the ionization potential (distance between vacuum energy and valence band maximum) of sputter deposited In_2O_3 amounts to $I_P = 7.1 \pm 0.15$ eV (see Table I and Ref. 49) in agreement with reactively evaporated In_2O_3 films,[28] while those of ITO films amounts to $I_P = 7.7 \pm 0.1$ eV (see Table I and Ref. 27). All ionization potentials determined from *in situ* deposited films are independent on the oxygen pressure during deposition indicating that the work function shifts are only due to different Fermi level positions.

Because of the expected influence of Sn we have evaluated its concentration at the surface from the XP spectra. Results for ITO films deposited at 400 °C substrate temperature with a different oxygen content in the sputter gas are shown in Fig. 6(a). The values are derived from integrated peak areas of background subtracted In $3d_{5/2}$ and Sn $3d_{5/2}$ core level spectra divided by sensitivity factors provided by the manufacturer of the XPS system.[50] The Sn concentration is calculated as $I(\mathrm{Sn})/[I(\mathrm{Sn}) + I(\mathrm{In})]$ and corresponds to the cation % of Sn. Error bars represent relative uncertainties, which are determined only from the accuracy of the core level intensities and are below ±5%. The relative uncertainty of the Sn content is much lower than the typical absolute uncertainty of composition analysis using XPS (5–10%), since only relative intensities of two cation core levels are compared.

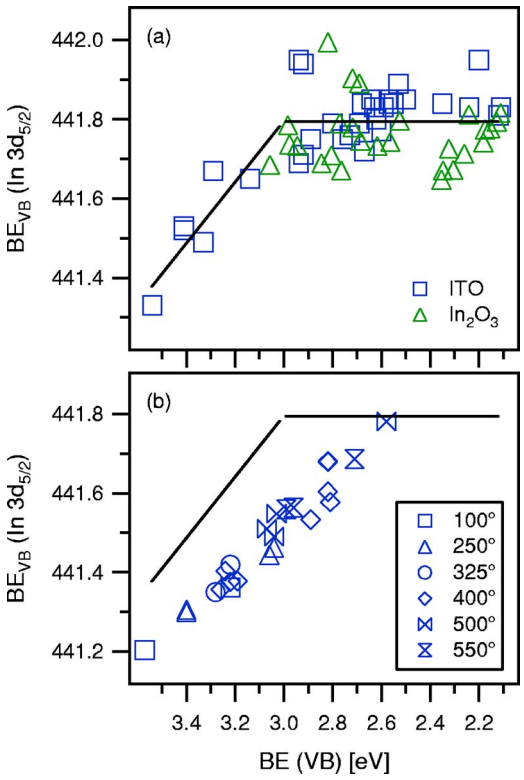

FIG. 5. (Color online) Binding energy with respect to the valence band maximum $\mathrm{BE_{VB}}$(In 3*d*) of In_2O_3 and ITO thin films in dependence on valence band maximum energy BE(VB) (a). The variation is induced by different deposition parameters. Low values of BE(VB) correspond to more oxidizing conditions. In (b) the same plot is shown for an ITO sample measured *in situ* during exposure to different atmospheres at different temperatures (indicated in °C). All binding energies are determined from the maximum of the emission line. The lines in (a) are drawn to show the anticipated dependence. Lines in (b) are reproduced from (a).

The data in Fig. 6(a) suggest an increase of Sn content at the surface above the target composition (9.2%) with higher Fermi level position (less oxygen content in the sputter gas). The behavior is highly reproducible. Although segregation of Sn at ITO surfaces has been reported in the literature,[24,51] the data in Fig. 6 indicate a correlation between the Fermi level position and the concentration of Sn at the surface.

B. *In situ* high-pressure measurements

Selected spectra recorded with $h\nu = 600$ eV synchrotron radiation from a clean ITO surface at different atmospheres

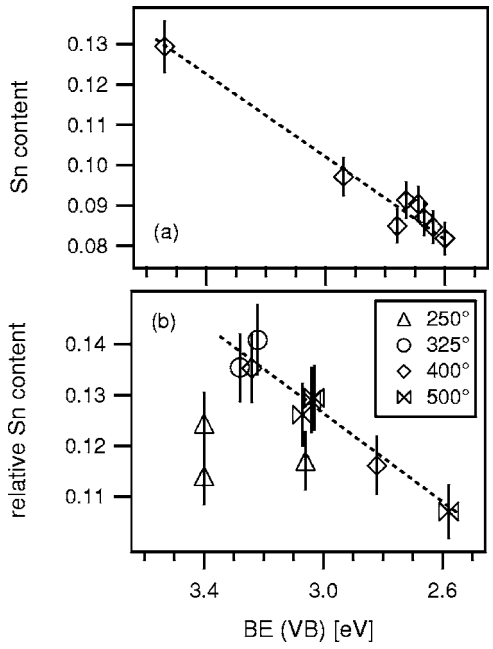

FIG. 6. Concentration of Sn determined from XP spectra of sputter deposited ITO films versus valence band maximum binding energy BE(VB). Low values of BE(VB) correspond to more oxidizing conditions. Values in (a) are absolute concentrations in cation % Sn $[I(\mathrm{Sn})/(I(\mathrm{Sn})+I(\mathrm{In})]$ determined *in situ* from samples after deposition of films. The films were deposited at 400 °C substrate temperature with varying oxygen content in the sputter gas. Values in (b) are relative concentrations determined from integrated intensities of core levels recorded with $h\nu=600$ eV synchrotron radiation of an ITO sample exposed to different environments at different substrate temperatures (indicated in °C). The lines are drawn to guide the eye.

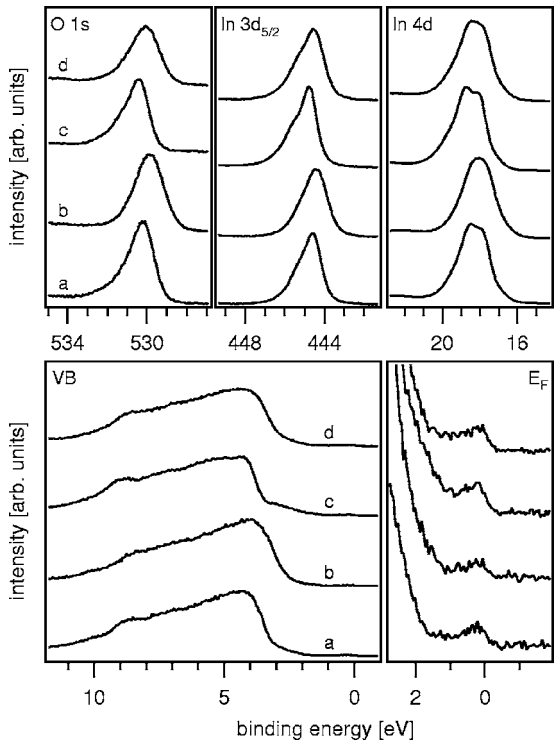

FIG. 7. Core level and valence band photoelectron spectra of an ITO sample hold at different temperatures and atmospheres. The spectra were recorded with $h\nu=600$ eV synchrotron radiation during exposure to 5×10^{-4} mbar oxygen (a,b) and 5×10^{-4} mbar hydrogen (c,d). Sample temperatures were 100 °C for (a) and (c) and 500 °C for (b) and (d), respectively. The spectra are normalized to the electron current in the storage ring and referenced to the Fermi edge emission of the sample.

and temperatures are shown in Fig. 7. The changes in the In $3d_{5/2}$, In $4d$, and O $1s$ core levels and in the valence band spectra are comparable to those described above for differently prepared films. A peak shape analysis of the In $4d$ level has not been performed, as it is more complicated than for the In $3d$ and O $1s$ levels because of the spin-orbit splitting and a shoulder occurring at low binding energies (see also Ref. 28). Nevertheless, the asymmetric peak shape seems to be more pronounced the higher the binding energy, in agreement with the analysis and interpretation given in the previous section. In contrast to the spectra shown in Fig. 3, peak analysis of the In $3d$ and O $1s$ spectra shown in Fig. 7 indicates a three-component structure as in Fig. 4 for all emissions, with varying widths of the peaks, indicating some differences in surface conditions compared to the freshly deposited samples.

The sample shows lower binding energies when exposed to oxygen compared to hydrogen exposed samples, corresponding to a partial oxidation and reduction of the sample. In contrast to the films deposited with a comparable oxygen partial pressure, a Fermi edge emission is clearly observed for all sample conditions (see Fig. 7). This suggests that the surface cannot be as strongly oxidized by exposure to O_2 gas, as it can be if films are deposited with addition of oxygen. The intensity of the Fermi edge is highest for spectra (c) and lowest for spectra (b) and therefore shows a tendency to increase with increasing binding energy of the spectra.

The binding energy of the In $3d_{5/2}$ core level with respect to the valence band maximum $\mathrm{BE_{VB}}$(In $3d$) recorded at different temperatures and gas atmospheres is plotted in Fig. 5(b). As for the freshly deposited samples, a clear dependence of $\mathrm{BE_{VB}}$(In $3d$) on the valence band maximum position is observed. However, the dependency does not agree quantitatively with the values obtained from freshly prepared samples, which are displayed in Fig. 5(a). The discrepancy might also be related to a different surface condition. This is suggested by the Fermi edge structure, which is observed for values of BE(VB) down to 2.6 eV in the high-pressure experiments. In contrast, the Fermi edge observed in UPS measurements disappears for $\mathrm{BE(VB)}\lesssim 3$ eV for the samples measured at room temperature directly after deposition.[26,27]

The Sn content at the surface has been evaluated from the integrated intensities of the Sn $3d_{5/2}$ and the In $3d_{5/2}$ emissions. No absolute determination is possible from these data, since the photoelectron excitation cross sections and the analyzer transmission both depend on energy. In addition, in the current experiment the sensitivity also depends on the gas pressure, since slower electrons are more strongly reduced at higher pressure. The effect is not considered to strongly affect the evaluation as the kinetic energies of electrons emitted from In $3d$ and from Sn $3d$ levels are comparable and

only data for pressures <0.1 mbar have been used, which have almost no effect on the count rate. Nevertheless, only a relative Sn content can be given, which is displayed in Fig. 6(b). It is evident that the Sn content changes reproducibly with surface condition. As for the freshly deposited samples there is a clear correlation between the concentration of Sn at the surface with the Fermi level position for sample temperatures $\geq 325\,^{\circ}\mathrm{C}$. This indicates sufficient mobility of Sn at this temperature. Only for a sample temperature of 250 °C the Sn concentration deviates from the observed general dependence, which is indicated in Fig. 6(b) by the dashed line. This line represents the Sn concentration expected for an equilibrium situation.

IV. DISCUSSION

We have presented measurements of surface properties of In_2O_3 and ITO by photoelectron spectroscopy with a special emphasis on the description of the surface potentials of these materials. Sputter deposited films were measured *in situ* directly after preparation and during gas exposure. The surfaces are free of carbon species and exhibit reproducible shifts of photoelectron binding energies with sample treatment. In addition a variation of core level to valence band maximum binding energy difference $BE_{VB}(CL)$ and of surface Sn concentration is observed. Both effects are obviously related to the Fermi level position. As a consequence of the variation in $BE_{VB}(CL)$, care must be taken when band bending changes are evaluated. A proper description of core level line shape in terms of screened and unscreened components as described in Sec. III A is required. Otherwise the band bending needs to be evaluated directly from the shifts of the valence band onset and not by the (smaller) shifts of the core levels. Changes in core level to valence band maximum binding energy differences will have to be considered whenever high densities of free carriers are involved as, e.g., for degenerately doped semiconductors, but also when the Fermi level is shifted into the conduction or valence band as a result of large interface charge redistribution.

The variation of $BE_{VB}(CL)$ might be directly related to the Sn content at the surface by formation of a distinct surface phase. This explanation, however, can be ruled out, since films prepared with 10% oxygen in the sputter gas also contain a considerable fraction of Sn [see Fig. 6(a)] but have the same $BE_{VB}(CL)$ as the In_2O_3 films [see Fig. 5(a) and Table I). In addition, the samples measured *in situ* at high pressures and lower temperatures (250 °C) have a nonequilibrium Sn concentration [see Fig. 6(b)], but the values of $BE_{VB}(CL)$ show no deviation from the almost linear dependence on the valence band maximum energy [see Fig. 5(b)].

The variation of $BE_{VB}(CL)$ observed for ITO is rather related to the screening of the core hole by free electrons, as indicated by the correlation of the variation in $BE_{VB}(CL)$ with the observation of a Fermi edge and the absence of the effect on In_2O_3 surfaces. The latter do not exhibit a clear Fermi edge emission. Thus, the presence of Sn appears to affect the occupation and/or the density of states around the Fermi energy at the surface considerably.

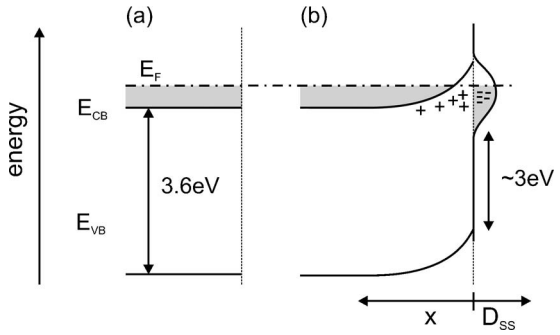

FIG. 8. Possible surface potential distributions leading to the observation of photoelectron emission at the Fermi level from a degenerately *n*-doped semiconductor. (a) Flat band situation: the Fermi level at the surface is inside the conduction band as in the bulk of the material; (b) Surface potential drop: the emission can only occur if a high density of surface states is present at the Fermi energy compensating for the space charge.

A Fermi edge emission can in principle occur for two different situations which are illustrated in Fig. 8. In (a) the Fermi level at the surface is above the conduction band minimum as in the bulk of the material. This is the common argument typically followed in the literature[16,22,24] and also typically assumed for contact properties, where ITO is usually treated like a metal.[11,15,52] In (b) there is a high density of surface states in the fundamental band gap and the Fermi energy crosses the surface band. Such a situation is, e.g., present at the $Si(111)7\times7$ surface.[53] Since the Fermi level is inside the conduction band in the bulk of the material, the bands must bend upwards in order to match a surface Fermi level inside the band gap. The positive space charge associated with this potential must be compensated by a negative charge in the surface states.

In contrast to literature, where the Fermi edge emission has been assigned to filled conduction band states as illustrated in Fig. 8(a) we attribute the metallic surface and the associated screening of the core holes in photoemission to a two-dimensional electron gas due to occupied surface states as illustrated in Fig. 8(b). The reasons for this are:

(1) A band gap above 4 eV is derived from optical absorption measurements with uncertainties below 0.1 eV for highly doped ITO films.[1,25] Hence the onset of the valence band maximum should occur at this energy. In contrast, even for the highest doping levels BE(VB) is never larger than 3.55 ± 0.05 eV (see Fig. 5 and Table I).

(2) The energy losses determined from the fits (see Fig. 4) occur at energies which are larger than the bulk plasmon energies for the highest doped ITO samples.[1] In contrast, in photoemission surface plasmons should contribute to the inelastic loss, which even have a lower energy than bulk plasmons.[45,54] The observed loss energies therefore suggest a different origin than a homogeneous electron gas.

(3) An ITO film deposited with 10% oxygen in the sputter gas shows a low Fermi energy and no Fermi edge emission. After deposition of the organic conductor Zn-Phthalocyanine (ZnPc), the Fermi level rises significantly towards the conduction band. Simultaneously, the Fermi edge emission reappears.[26,27]

(4) One of the strongest arguments for the presence of a carrier depletion layer at ITO surfaces is the observed Sn segregation and particularly the correlation of the surface Sn concentration with a change of the surface Fermi level position. Segregation of dopant atoms at ITO surfaces has already been identified in the past using XPS measurements.[24,51] Cox *et al.* have calculated a thermodynamical heat of segregation from different Sn contents obtained after different sample treatments.[24] In contrast, our results suggest that the surface Sn content is directly related to the surface Fermi level position (see Fig. 6), which can be explained by variations of defect concentrations in the presence of space charges.[55] Since Sn substituting for In is a donor, its charge state is either neutral or positive, depending on the Fermi level position. Since Sn can be used for degenerate doping of In_2O_3, its charge transition energy can be assumed to be inside or at least close to the conduction band. Therefore most of the Sn near the surface should be positively charged and will therefore be Coulomb attracted by the negative surface charge. In case of a homogeneous situation there would be no electrostatic driving force for segregation and a chemical driving force is not considered to be reversible when the surface potential changes. Hence, for the homogeneous situation displayed in Fig. 8(a) no electronically driven segregation of Sn is expected.

In general, at higher temperature the surface will be more reduced, which, according to Fig. 6, should result in a higher Sn content in agreement with the reported data.[24] However, it is also evident that the surface Sn content can noticeably change on a time scale of an hour at temperatures as low as 300 °C. Consequently, not only the treatment temperature but also the details of the cooling procedure will affect the Sn concentration. Of course the details of the temperature treatment will not only affect the surface but also the bulk properties of the material (for a description of such mechanisms see, e.g., Ref. 56).

The observation of metallic states at ITO surface appears to be related to the presence of Sn. This is indicated by the absence of a Fermi edge emission and the constant BE_{VB}(CL) values on In_2O_3 surfaces. Surface states on SnO_2 and In_2O_3 surfaces have been reported in the literature and are due to undercoordinated (unsaturated) metal atoms.[28,42–47] The surface states are therefore mainly derived from Sn or In 5*s* orbitals, which in the bulk mainly contribute to the conduction band. Surprisingly, reduced surfaces of SnO_2 and In_2O_3 show emission from surface states in the lower half of the band gap close to the valence band rather than near the conduction band.[28,45,46] This effect has been attributed to hybridization between 5*s* and 5*p* states.[43,45,47] A similar effect might occur at surfaces of In_2O_3, which also show surface states close to the valence band.[28] Also reduced ITO surfaces show this emission (see Figs. 3 and 7). Placing a Sn atom at an In surface site results in a different situation as an additional electron is now available. This might lead either to different filling of the surface states and/or to a different reorganization of the surface followed by a modified electronic structure. Theoretical investigations of the electronic structure of ITO surfaces in comparison to those of In_3O_3 might clarify this point. Taking the data presented in Fig. 5(a) we suggest that the ITO surface exhibits a surface band with a lower edge 3 eV above the valence band maximum, as indicated in Fig. 8(b). The structure might be the same for In_2O_3. However, the In_2O_3 films investigated by us are not highly enough doped to give rise to a Fermi level position noticeably above the minimum of the surface band.

For completeness it is mentioned that for highly degenerate semiconductors as ITO space charge layers are expected to be very thin. Segregation of Sn donors would increase the surface doping and further reduce the thickness of the space charge layer. This contrasts energy dependent photoemission measurements and has been related to the presence of a surface layer with a reduced doping at In_2O_3 and ITO surfaces.[25,29] Such a *chemical depletion layer* is in agreement with the observation of an increased oxygen content in nanocrystalline ITO.[57] It is not associated with a space charge and therefore also not to charged surface states. The presence of the chemical depletion layers at In_2O_3 and ITO surfaces does not affect any conclusion presented here. The observation of Sn segregation, e.g., is only related to the *physical depletion layer* which results from the variation of the electrostatic potential due to the presence of the space charge layer which balances the charge in the surface states. This is particularly evident from the correlation of the Sn content with the surface Fermi level position (occupation of the surface states). Chemical depletion layers have therefore been neglected throughout this paper and will be described in more detail elsewhere.

The presence of a high density of surface states also explains the apparent differences in observed band gaps as outlined in the Introduction. A different Fermi level position at the surface (and grain boundary) of the film gives rise to a different absorption edge. The absorption edge at the surface is determined by the distance between the valence band maximum and the Fermi energy [$E_F - E_{VB}$ or BE(VB)]. The measured values for BE(VB) are in good agreement with the "indirect" gaps of In_2O_3 and ITO reported in the literature.[30,31]

V. SUMMARY AND CONCLUSIONS

Surface properties of radio-frequency magnetron sputter deposited In_2O_3 and ITO thin films were investigated by *in situ* photoelectron spectroscopy. Measurements were performed either directly after thin film deposition without exposing samples to air, or during exposure to different gas environments after a surface cleaning by heating samples which has been stored in air. Depending on sample preparation and treatment, systematic changes of binding energies are observed being due to changes of the surface Fermi level position.

ITO (and probably also In_2O_3) shows surface states in the upper half of the band gap. The surface states have multiple consequences: (i) ITO surfaces exhibit a surface Fermi level position inside the fundamental gap. The observed Fermi edge emission is explained by emission from surface states rather than from filled conduction band states. (ii) For significant filling of the surface state band, screening of the core

hole reduces the binding energies of the In 3*d* and O 1*s* core levels with respect to the valence band maximum. Because of this variation it is not possible to deduce the shifts of the Fermi level position at the surface directly from the core level binding energy shifts. (iii) As a consequence of the negative charge associated with the surface states, segregation of Sn to the surface occurs. The concentration of Sn at the surfaces shows a direct correlation with the surface Fermi level position. In addition Sn is obviously mobile enough in ITO to change its surface concentration on the time scale of an hour at $T \approx 300\ ^\circ\mathrm{C}$. (iv) It is suggested that the surface states are responsible for the occasionally reported indirect band gaps of In_2O_3 and ITO.

ACKNOWLEDGMENTS

The presented work was funded by the German Science Foundation via the collaborative research center SFB 595 (Electrical Fatigue in Functional Materials). We also acknowledge financial support from BESSY during beamtime at the synchrotron.

*Electronic address: Email address: aklein@surface.tu-darmstadt.de

[1] I. Hamberg and C. G. Granqvist, J. Appl. Phys. **60**, R123 (1986).
[2] H. L. Hartnagel, A. L. Dawar, A. K. Jain, and C. Jagadish, *Semiconducting Transparent Thin Films* (Institute of Physics Publishing, Bristol, 1995).
[3] G. Frank and H. Köstlin, Appl. Phys. A **27**, 197 (1982).
[4] G. B. González, J. B. Cohen, J.-H. Hwang, T. O. Mason, J. P. Hodges, and J. D. Jorgensen, J. Appl. Phys. **89**, 2550 (2001).
[5] J.-H. Hwang, D. D. Edwards, D. R. Kammler, and T. O. Mason, Solid State Ionics **129**, 135 (2000).
[6] T. O. Mason, G. B. González, J. H. Hwang, and D. R. Kammler, Phys. Chem. Chem. Phys. **5**, 2183 (2003).
[7] L. S. Hung and C. H. Chen, Mater. Sci. Eng., R. **39**, 143 (2002).
[8] C. J. Brabec, N. S. Sariciftci, and J. C. Hummelen, Adv. Funct. Mater. **11**, 15 (2001).
[9] P. Peumans, A. Yakimov, and S. R. Forrest, J. Appl. Phys. **93**, 3693 (2003).
[10] N. G. Patel, P. D. Patel, and V. S. Vaishnav, Sens. Actuators B **96**, 180 (2003).
[11] H. Ishii, K. Sugiyama, E. Ito, and K. Seki, Adv. Mater. (Weinheim, Ger.) **11**, 605 (1999).
[12] D. Kohl, J. Phys. D **34**, R125 (2001).
[13] W. Jaegermann, in *Modern Aspects of Electrochemistry*, edited by R. E. White (Plenum Press, New York, 1996), Vol. 30, pp. 1–185.
[14] F. Nüesch, L. J. Rothberg, E. W. Forsythe, Q. T. Le, and Y. Gao, Appl. Phys. Lett. **74**, 880 (1999).
[15] T. Kugler, W. R. Salaneck, H. Rost, and A. B. Holmes, Chem. Phys. Lett. **310**, 391 (1999).
[16] M. G. Mason, L. S. Hung, C. W. Tang, S. T. Lee, K. W. Wong, and M. Wang, J. Appl. Phys. **86**, 1688 (1999).
[17] I. G. Hill, D. Milliron, J. Schwartz, and A. Kahn, Appl. Surf. Sci. **166**, 354 (2000).
[18] K. Sugiyama, H. Ishii, Y. Ouchi, and K. Seki, J. Appl. Phys. **87**, 295 (2000).
[19] J. S. Kim, B. Lägel, E. Moons, N. Johansson, I. D. Baikie, W. R. Salaneck, R. H. Friend, and F. Cacialli, Synth. Met. **111**-112, 311 (2000).
[20] J. A. Chaney and P. E. Pehrsson, Appl. Surf. Sci. **180**, 473 (2001).
[21] C. Donley, D. Dunphy, D. Paine, C. Carter, K. Nebesny, P. Lee, D. Alloway, and N. R. Armstrong, Langmuir **18**, 450 (2002).
[22] V. Christou, M. Etchells, O. Renault, P. J. Dobson, O. V. Salata, G. Beamson, and R. G. Egdell, J. Appl. Phys. **88**, 5180 (2000).
[23] K. H. Lee, H. W. Jang, K.-B. Kim, Y.-H. Tak, and J.-L. Lee, J. Appl. Phys. **95**, 586 (2004).
[24] P. A. Cox, W. R. Flavell, and R. G. Egdell, J. Solid State Chem. **68**, 340 (1987).
[25] Y. Gassenbauer and A. Klein, Solid State Ionics **173**, 141 (2004).
[26] D. Ensling, A. Thissen, Y. Gassenbauer, A. Klein, and W. Jaegermann, Adv. Eng. Mater. **7**, 945 (2005).
[27] Y. Gassenbauer and A. Klein, J. Phys. Chem. B **110**, 4793 (2006).
[28] A. Klein, Appl. Phys. Lett. **77**, 2009 (2000).
[29] A. Klein, Mater. Res. Soc. Symp. Proc. **666**, F1.10 (2001).
[30] R. L. Weiher and R. P. Ley, J. Appl. Phys. **37**, 299 (1966).
[31] F. Matino, L. Persano, V. Arima, D. Pisignano, R. I. R. Blyth, R. Cingolani, and R. Rinaldi, Phys. Rev. B **72**, 085437 (2005).
[32] E. Burstein, Phys. Rev. **93**, 632 (1954).
[33] T. S. Moss, Proc. Phys. Soc. London, Sect. B **67**, 775 (1954).
[34] I. Hamberg, C. G. Granqvist, K.-F. Berggren, B. E. Sernelius, and L. Engström, Phys. Rev. B **30**, 3240 (1984).
[35] O. N. Mryasov and A. J. Freeman, Phys. Rev. B **64**, 233111(R) (2001).
[36] A. Klein, Adv. Solid State Phys. **44**, 13 (2004).
[37] M. Marezio, Acta Crystallogr. **20**, 723 (1966).
[38] D. R. Batchelor, R. Follath, and D. Schmeisser, Nucl. Instrum. Methods Phys. Res. A **467-468**, 470 (2001).
[39] D. Teschner, A. Pestryakov, E. Kleimenov, M. Haevecker, H. Bluhm, H. Sauer, A. Knop-Gericke, and R. Schloegl, J. Catal. **230**, 186 (2005).
[40] E. Kleimenov, H. Bluhm, M. Haevecker, A. Knop-Gericke, A. Pestryakov, D. Teschner, J. A. Lopez-Sanchez, J. K. Bartley, G. J. Hutchings, and R. Schloegl, Surf. Sci. **575**, 181 (2005).
[41] G. V. Rao, F. Säuberlich, and A. Klein, Appl. Phys. Lett. **87**, 032101 (2005).
[42] V. Golovanov, M. A. Mäki-Jaskari, T. T. Rantala, G. Korotcenkov, V. Brinzari, A. Cornet, and J. Morante, Sens. Actuators B **106**, 563 (2005).
[43] P. A. Cox, R. G. Egdell, C. Harding, W. R. Patterson, and P. J. Taverner, Surf. Sci. **123**, 179 (1982).
[44] D. F. Cox, T. B. Fryberger, and S. Semancik, Phys. Rev. B **38**, 2072 (1988).
[45] R. G. Egdell, J. Rebane, T. J. Walker, and D. S. L. Law, Phys. Rev. B **59**, 1792 (1999).
[46] J. M. Themlin, R. Sporken, J. Darville, R. Caudano, J. M. Gilles, and R. L. Johnson, Phys. Rev. B **42**, 11914 (1990).

[47] I. Manassidis, J. Goniakowski, L. N. Kantorovich, and M. J. Gillan, Surf. Sci. **339**, 258 (1995).
[48] J.-N. Chazalviel, M. Campagna, G. K. Wertheim, and H. R. Shanks, Phys. Rev. B **16**, 697 (1977).
[49] R. Schafranek, Master's thesis, Technische Universität Darmstadt (2004).
[50] J. F. Moulder, W. F. Stickle, P. E. Sobol, and K. D. Bomben, *Handbook of X-ray Photoelectron Spectroscopy* (Physical Electronics, Inc., Eden Prairie, 1995).
[51] J. C. C. Fan and J. B. Goodenough, J. Appl. Phys. **48**, 3524 (1977).
[52] I. G. Hill and A. Kahn, J. Appl. Phys. **86**, 2116 (1999).
[53] W. Mönch, *Semiconductor Surfaces and Interfaces* (Springer Verlag, Heidelberg, 1993).
[54] V. E. Henrich and P. A. Cox, *The Surface Science of Metal Oxides* (Cambridge University Press, Cambridge, 1994).
[55] J. Maier, Prog. Solid State Chem. **23**, 171 (1995).
[56] J. Maier, Phys. Chem. Chem. Phys. **5**, 2164 (2003).
[57] G. B. González, T. O. Mason, J. P. Quintana, O. Warschkow, D. E. Ellis, J.-H. Hwang, and J. P. Hodges, J. Appl. Phys. **96**, 3912 (2004).